Water-suppression cycling (WSC) 3T cardiac ^{1}H-MRS detects altered creatine and choline in patients with aortic or mitral stenosis

Belinda Ding,[1,2] Mark Peterzan,[2] Ferenc E. Mózes,[2] Oliver J. Rider,[2] Ladislav Valkovič[2,3], Christopher T. Rodgers[1,2]

[1]Wolfson Brain Imaging Centre, University of Cambridge, Box 65, Cambridge Biomedical Campus, Cambridge, CB2 0QQ, UK

[2]Oxford Centre for Clinical Magnetic Resonance Research (OCMR), University of Oxford, Level 0, John Radcliffe Hospital, Oxford, OX3 9DU, UK

[3]Department of Imaging Methods, Institute of Measurement Science, Slovak Academy of Sciences, Bratislava, Slovakia

Word count: 6915 words (in main body of text)

Proofs to be sent to:

Belinda Ding
Wolfson Brain Imaging Centre,
University of Cambridge,
Cambridge Biomedical Campus Box 65,
Cambridge,
CB2 0QQ
United Kingdom

Email: ybd21@cam.ac.uk

Keywords

Water-suppression cycling; heart; cardiac; ^{1}H-MRS; 3T; human; STEAM; PRESS

Abstract (word count: 292, word limit: 300)

Cardiac proton spectroscopy (^{1}H-MRS) is widely used to quantify lipids. Other metabolites, e.g. creatine and choline, are clinically relevant but more challenging to quantify because of their low concentrations (~10 mmol/L) and because of cardiac motion.

To quantify cardiac creatine and choline, we added water-suppression cycling ('WSC') to two single voxel spectroscopy sequences (STEAM and PRESS). WSC introduces controlled residual water signals that alternate between positive and negative phase from transient to transient, enabling robust phase and frequency correction. Moreover, a particular weighted sum of transients eliminates residual water signals without baseline distortion.

We compared WSC and the vendor's standard "WET" water-suppression in phantoms. Next, we tested repeatability in 10 volunteers (7 male; 29.3±4.0 years; BMI 23.7±4.1 kg/m^2). Fat fraction, creatine concentration and choline concentration when quantified by STEAM-WET were 0.30±0.11%, 29.6±7.0 μmol/g and 7.9±6.7 μmol/g respectively; and when quantified by PRESS-WSC they were 0.30±0.15%, 31.5±3.1 μmol/g and 8.3±4.4 μmol/g respectively. Compared to STEAM-WET, PRESS-WSC gave spectra whose fitting quality expressed by Cramér-Rao bounds improved by 26% for creatine and 32% for choline. Repeatability of metabolite concentration measurements improved by 72% for creatine and 40% for choline.

We also compared STEAM-WET and PRESS-WSC in 13 patients with severe symptomatic aortic or mitral stenosis indicated for valve replacement surgery (10 men; 75.9±6.3 years; BMI 27.4±4.3 kg/m^2). Spectra were of analysable quality in 8 patients for STEAM-WET, and 9 for PRESS-WSC. We observed comparable lipid concentrations to those in healthy volunteers, significantly reduced creatine concentrations, and a trend towards decreased choline concentrations.

We conclude that PRESS-WSC offers improved performance and reproducibility for quantification of cardiac lipids, creatine and choline concentrations in healthy volunteers at 3T. It also offers improved performance compared to STEAM-WET for detecting altered creatine and choline concentrations in patients with valve disease.

List of abbreviations

ADP	adenosine diphosphate
ATP	adenosine triphosphate
Cho	choline
CK	creatine kinase
Cr	creatine
CRLB	Cramér-Rao lower bounds
HLSVD	Hankel Lanczos singular value decomposition
MAD	median absolute deviations
OXSA	Oxford Spectroscopy Analysis (open-source MATLAB toolbox)
PCr	phosphocreatine
P_i	inorganic phosphate
PRESS	point resolved spectroscopy
STEAM	stimulated echo acquisition mode
WET	water suppression enhanced through T_1 effects
WSC	water-suppression cycling

Introduction

Magnetic resonance spectroscopy (^{1}H-MRS) is an established method to assess metabolite concentrations in the human heart. In diseases, such as obesity and type-II diabetes, the heart's uptake and oxidation of fatty acids are not balanced, resulting in an accumulation of triglycerides.[1] The accumulation of triglycerides leads to metabolic derangement, which has been proposed as a contributory and/or perpetuating factor in non-ischaemic cardiomyopathies.[1,2] Therefore, most published cardiac ^{1}H-MRS studies have focused on quantifying lipid concentrations.[3–5] However, with sufficient data quality, ^{1}H-MRS can also assess lower concentration metabolites such as creatine (Cr) and choline† (Cho) that are of high clinical interest.[6–8]

Creatine is an important component in the creatine kinase (CK) enzyme system.[9] CK catalyses the transfer of a high-energy phosphate group from adenosine triphosphate (ATP) onto creatine to form phosphocreatine and adenosine diphosphate (ADP) in the mitochondria:

$$\mathrm{ATP} + \text{free Cr} \rightleftharpoons \mathrm{ADP} + \mathrm{PCr} \qquad (1)$$

In the myofibrils, the reverse reaction provides a very rapid supply of ATP to meet demand during bursts of effort such as sustaining contraction throughout systole.[10,11] These ATP-delivery processes become deranged in heart failure, according to the energy-starvation hypothesis.[12] In failing human and animal hearts, free creatine and phosphocreatine concentrations drop substantially soon after disease onset[13] and before failure of ATP homeostasis.[9,14] Note that in vivo, the free Cr and PCr ^{1}H-MRS peaks are overlapping. It is therefore common to report 'total creatine' (tCr), defined as the sum of free Cr and PCr. Creatine concentrations obtained via ^{1}H-MRS can be used to calculate the heart's energy reserve ($|\Delta G_{ATP}|$),[15,16] which in turn can predict isovolumic contractile reserve[17] and peak cardiac work.[18,19] Hence, a decrease in $|\Delta G_{ATP}|$ limits the heart's maximum mechanical work and eventually a reduced $|\Delta G_{ATP}|$ could lead to heart failure. On top of that, $|\Delta G_{ATP}|$ is a potential biomarker that could be used to evaluate novel 'energy sparing' treatments for heart failure, e.g. drugs that modulate fatty acid oxidation such as etomoxir[20] and perhexiline.[21]

Cholines are a class of quaternary ammonium salts that serve several physiological functions such as maintaining structural integrity in cell membranes and facilitating cell membrane signalling.[22] The choline derivative acetylcholine is an important neurotransmitter in the autonomic nervous system, which regulates heart rate and blood pressure,[23] and in the brain, where defective cholinergic signalling is implicated in Alzheimer's dementia.[24] Cholines have also been identified as a potential biomarker for

† The peak we refer to as "choline" for brevity may also contain taurine and carnitine. It is denoted by some authors as the "trimethylammonium (TMA) containing compounds" peak.

identifying active tumours, e.g. in the brain,[25] breast,[26] and liver.[27] However, whether myocardial choline levels change in disease is still poorly understood in both animal models and humans.

Thus far, most in vivo cardiac ^{1}H-MRS studies have used single voxel spectroscopy (SVS) techniques such as STimulated Echo Acquisition Mode (STEAM) and Point RESolved Spectroscopy (PRESS) together with a pulse sequence module that suppresses water signals.[28] Patient motion, including respiration and cardiac motion mean that there can be phase and frequency shifts between each transient recorded by the scanner. This can cause incoherent averaging during post-processing, and hence reduce signal to noise ratio (SNR). A common approach for both cardiac and brain spectroscopy involves phasing and frequency shifting individual transients using the largest peak (residual water or a metabolite).[3,28–32] To ensure that there is a sufficiently large reference peak for frequency and phase correction, many studies only partially suppress water (so called 'weak water suppression').[28,29] However, with weak water suppression, the residual water peak can still cause problems during spectral fitting.[33]

In this work, we propose instead to use a water-suppression cycling (WSC) method[34], originally developed for brain ^{1}H-MRS, to improve the quality of cardiac single-voxel ^{1}H-MRS at 3 T. The WSC technique inserts a weak water suppression module and adds an inversion pulse in alternate transients. The weak water suppression property of this module provides a high SNR residual water peak for frequency and phase correction, while inverting the residual water signal every other scan allows for practically complete elimination of the residual water peak during post-processing (as we show below) which improves spectral fitting, e.g. by avoiding errors from baseline distortion. WSC is similar conceptually to the method known as "metabolite cycling",[7,35] except that during metabolite cycling it is the metabolite peaks that are inverted, whereas WSC only inverts the residual water peak.

Here we aimed to test the feasibility of the WSC approach to improve quantification of low-concentration metabolites such as creatine and choline (as well as lipids) in the heart at 3T; and to investigate potential changes in cardiac creatine and choline levels in patients with valvular stenosis.

This is a particularly exciting, but as-yet under-investigated group of patients, in which 15% of patients undergoing surgical aortic valve replacement have reduced left ventricular ejection fraction (<50%).[38] However, at present it is not possible to anticipate or explain why the myocardium in some patients but not others exhibits contractile decline in the face of sustained severe pressure overload. Nonetheless, otherwise unexplained contractile decline into the borderline (LVEF 50-59%) range worsens prognosis[38–40] and, in the absence of good understanding regarding the underlying mechanism, there is currently no specific medical therapy other than to refer for timely valve replacement once the valve disease has progressed into the severe range. The metabolic hypothesis of heart failure posits that reduced metabolic reserve is both a permissive and a causative factor at play, and while there are many animal models that support this,[41,42] the evidence in human pressure overload hypertrophy is sparser[13,43]

because of the difficulty in obtaining human myocardium and because there are few established techniques for non-invasive myocardial metabolic phenotyping. Despite the known association between reduced phosphocreatine/ATP ratio and pathological left ventricular hypertrophy, there is mixed evidence regarding whether total creatine itself is reduced in this setting,[43–47] yet this would be a key variable to establish if one is to estimate the concentration of free ADP from the CK equilibrium expression and thereby come to an estimate of the free energy of ATP hydrolysis.

Theory

Water-suppression cycling

The water-suppression cycling ('WSC') module was first implemented by Ernst and Li for ^{1}H-MRS in the brain.[34] This technique alternates between positive and negative residual water signal every other transient. The residual water signal can be used to correct for phase and frequency shifts in single shots and its alternating phase allows for the elimination of the water peak upon post processing.

The implementation of the pulse sequence and the post-processing of each transient is presented in Figure 1. WSC is an interleaved method. The WSC module comprises four chemical shift selective RF pulses spaced 50 ms apart for partial water suppression prior to a standard single voxel pulse sequence such as PRESS or STEAM. Each RF pulse is a Gaussian with a time-bandwidth product of 0.896 centred on water and the spoiler gradients between pulses suppress residual transverse magnetisation (M_{xy}).[34] The third pulse in the module, a 180° chemical shift selective inversion pulse, is activated in odd numbered acquisitions and disabled in even numbered acquisitions, yielding two different spectra S_{odd} and S_{even}. This alternation results in the residual water and metabolite peaks having the same phases in S_{odd} and opposite phases in S_{even}.

Three corrections were applied before the odd and even numbered acquisitions were averaged together. First, frequency correction was performed to correct for minor frequency differences between the water signals in each transient. Second, a zero-order phase correction was performed based on the phase of the residual water peak to make it positive real in even transients and negative real in odd transients. Third, a weighting factor w that compensates for T_1 relaxation of the water signal and imperfections in the inversion pulses was determined by least-squares fitting such that spectra summed according to Eq 2 have minimum residual water signal. Finally, the odd and even spectra were averaged using Eq 2 where the denominator ensures that metabolite amplitudes remain unchanged (see SI Figure 1 for simulation results).

$$S = \frac{S_{odd} + w \times S_{even}}{1 + w} \quad (2)$$

In many ways, the WSC approach is similar to the method of "metabolite cycling"[35]. However, WSC has potential advantages that the residual water peak is eliminated before spectral fitting, and that

because metabolites are not inverted WSC may be less sensitive to the T_1 values of metabolites and the efficiency of the inversion pulse, as shown in Ernst & Li's original study.[34]

Methods

All data were collected using a whole-body clinical 3 T Prisma MRI scanner (Siemens Healthineers, Erlangen, Germany) with an 18-channel cardiac receive array coil (Siemens Healthineers) and a 32-channel spine receive array coil (Siemens Healthineers).

^{1}H MRS sequence

We compared the vendor's standard "water suppression enhanced through T_1 effects" (WET)[48] water suppression module against the WSC module described above. This gave four different protocols:

1. STEAM-WET
2. PRESS -WET
3. STEAM-WSC
4. PRESS-WSC

To minimize the loss of signal due to T_2 decay, we also modified the gradient slew rates and amplitudes to achieve shorter echo times for all four sequences (26 ms for PRESS and 10 ms for STEAM). On top of that, in order to improve performance of the vendor's WET water suppression for in vivo scans, we followed the procedure of Rial et al.[3] and used an additional breath-held pre-scan to manually optimise the water suppression flip angles.

Data acquisition

Phantom study

A phantom study was conducted to validate the ability to quantify creatine concentrations for each sequence together with its post processing steps in the absence of motion. A six-compartment phantom was prepared in a silicone ice cube tray with varying concentrations of creatine (SI Figure 2). The following were added to each compartment: agar (Sigma-Aldrich; 2.3% w/w), NaCl (Sigma-Aldrich; 43 mmol/L), sodium dodecyl sulphate (Sigma-Aldrich; 43 mmol/L), $NiCl_2$ (Sigma-Aldrich; 0.89 mmol/L), peanut oil (Tesco, UK; 1% v/v), and creatine (Sigma-Aldrich; 0, 5, 10, 20, 40 and 80 mmol/L). The mixture was heated to boiling point until the agar dissolved completely and the solution turned clear (around 30 minutes), then left to set overnight.

Spectra were acquired from the phantom from a 20 × 20 × 20 mm^3 voxel in the centre of each compartment after B_0 shimming with the vendor's 'Standard' method over an adjustment volume of 40 × 40 × 40 mm^3. For each compartment, 30 individual water-suppressed and 3 non-water-suppressed measurements (i.e. shots) were obtained with STEAM and PRESS using the product WET water suppression and product WET calibration, and then again using WSC water suppression (i.e. all four combinations). For non-water-suppressed acquisitions, only the gradients were active in the water-

suppression module (WSC or WET), and not the RF pulses. Acquisition parameters were: 1024 points, 2 kHz bandwidth, 4 s TR, 10 ms TE for STEAM and 26 ms TE for PRESS, 50 Hz water suppression pulse bandwidth. The scanner centre frequency was set at water (4.7 ppm) for non-water-suppressed acquisitions and the methyl group in creatine (3.0 ppm) for water-suppressed acquisitions.

Reproducibility study in healthy volunteers

10 healthy volunteers (7 men, 3 women; mean age ± standard deviation (SD) = 29.3 ± 4.0 years; age range = 23 – 34 years; BMI = 23.7 ± 4.1 kg/m^2) were recruited for this study and gave informed consent in accordance with local ethics regulations.

For each session, the volunteers were positioned head-first supine in the scanner with ECG gating (Siemens). Cine images were used to obtain horizontal long axis and short axis views of the heart. The MRS voxel was placed in the mid interventricular septum, to minimise the chance of contamination from epicardial fat. The trigger delay was adjusted for mid-diastole where cardiac motion is minimised,[49] usually around 650 ms for an average R-R interval of 1000 ms. B_0 shimming with the vendor's 'Heart' method was performed over an adjustment volume of 40 × 32 × 30 mm^3 during a breath hold. ^{1}H-MRS data were obtained at end-expiration from a 32 × 26 × 22 mm^3 voxel centred on the septum (Figure 2). This voxel contains more ventricular blood compared to previous studies that used smaller voxels (2 cm^3 – 8 cm^3),[50–56] but both STEAM and PRESS have been demonstrated to have dark blood properties[3,50,51] so contamination from the blood pool should not be significant.[57]

Due to institutional limits on scan durations and the challenge of repeated breathholds, it was not possible to run all four sequences. An initial experiment was conducted with six healthy volunteers (three women; age = 32.5 ± 6.2 years; age range = 25 – 42 years; body mass index (BMI) = 23.1 ± 1.97 kg/m^2) to compare PRESS-WET (150 measurements over 30 breathholds) and STEAM-WET (150 measurements over 30 breathholds). On the basis of this preliminary study, PRESS-WET was excluded from the later in vivo comparison (see SI Figure 2 for spectra and SI Table 1 for SNR, CRLB and linewidths for the preliminary study). Thus, in the main study, three sequences were run on the volunteers: STEAM-WET, STEAM-WSC and PRESS-WSC. Parameters for all three sequences matched the phantom experiment, with the following changes: 2 s TR for water-suppressed acquisitions and water-suppression bandwidth for WSC module was set at 65 Hz. For STEAM-WET, 150 water-suppressed spectra were acquired over 30 breathholds and 3 non-water-suppressed spectra were acquired over 1 breathhold to give a high quality "reference" data set.

For STEAM-WSC and PRESS-WSC, 60 water-suppression cycled spectra (i.e. 30 pairs) were acquired over 10 breathholds and 3 water-non-suppressed spectra were acquired over 1 breathhold. Across all sequences, each breathhold was between 11 – 13 s long, and a 13 – 20 s pause was given between each breathhold. Each session took around 1 hour in total.

To obtain repeatability data, each volunteer was scanned in two different sessions on the same day. They were taken out of the scanner between sessions, given a five-minute break, and the scan protocol was repeated. Total scan time for each volunteer was just over two hours including the repeat session. However, the large number of breathholds and long scan times were challenging for some volunteers. Based on an interim analysis of data from the first session in the first three volunteers, the STEAM-WSC was not repeated in the second session for the remaining volunteers.

In vivo study in patients

Thirteen patients (ten male, three female; age = 75.9 ± 6.3 years; age range = 63 – 83 years; BMI = 27.4 ± 4.3 kg/m^2) with severe symptomatic aortic or mitral stenosis were recruited as part of a project approved by regional (South Central Oxford C, 16/SC/0323) and local ethics and governance panels. Out of the group, eight patients had aortic stenosis with preserved left ventricular ejection fraction, three had aortic stenosis with reduced ejection fraction and one had mitral stenosis. The inclusion criteria were: age 18-85, with severe aortic stenosis and due to undergo clinically-indicated aortic valve replacement, or no pressure- or volume-loading valve disease (ie no hypertrophy) but due to undergo cardiac surgery and willing to donate cardiac biopsy; and the exclusion criteria were: prior myocardial infarction, flow-limiting coronary disease, more than mild bystander valve disease, renal impairment (eGFR <30 ml/min), or contra-indication to MRI scanning. A table summarising the patient demographics is included in the supplementary information (SI Table 2).

For each patient, 150 measurements (30 breathholds) were obtained with the STEAM-WET sequence as the STEAM-WET-150 "reference" data set and 60 measurements (10 breathholds) were obtained with the PRESS-WSC sequence.

Data analysis

Data post-processing

Signals from individual coil elements for each shot were combined and averaged using MATLAB (Mathworks Inc, Natick, MA). Weighting and phase correction factors for each coil were calculated from the water peak in the non-water-suppressed spectra and applied to the water-suppressed spectra.[3,58]

The spectrum from each transient was phase and frequency corrected based on either the lipid peak (for STEAM-WET and PRESS-WET) or the residual water peak (STEAM-WSC and PRESS-WSC) before averaging. A more detailed explanation of the post-processing steps for WSC sequences can be found in the Theory section and in Figure 1. All spectra were analysed using the OXSA toolbox[59]. For the creatine-fat phantom, five Lorentzian peaks were fitted: residual water around 4.7 ppm, Cr CH_2 peak around 3.9 ppm, Cr CH_3 peak around 3.0 ppm and two lipid peaks around 1.28 ppm and 0.84 ppm. For in vivo WET water-suppressed spectra, residual water signals were removed with the Hankel-Lanczos singular value decomposition (HLSVD) method.[60,61] The resulting spectra were fitted with 7 peaks: residual water, two peaks for the methyl and methylene group of total creatine at 3.0 ppm and 3.9 ppm;

a peak for the methyl group of choline derivatives at 3.2 ppm; and three peaks for lipids chains at 1.99 ppm (allylic), 1.28 ppm (methylene) and 0.84 ppm (methyl).[4] Note that although we fit two peaks for creatine, we used only the creatine CH_3 signal at 3.0 ppm for analysis of total creatine. In this paper, we used 'choline' to refer to any trimethylammonium (TMA) compound as used by Gillinder et al.[6], however, the peak is likely to include contributions from other nitrogen-containing compounds such as carnitine or taurine. Each raw transient, intermediate outputs from the post processing pipeline and the final fittings were all visually inspected for potential errors.

Across all spectra, the SNR of each peak was estimated by taking the ratio of the peak height in a 10 Hz exponentially apodized spectrum (matched filtering) to the standard deviation of the noise extracted from the Fourier transform of the last 100 points of the free induction decay of the filtered spectrum.[62] Note that care must be taken when comparing spectroscopy SNR values *between* studies because there are many slightly different definitions of SNR. The accuracy of the spectral fitting was estimated by calculating the Cramér-Rao Lower Bounds (CRLB).[63] Due to time constraints, we were unable to run 150 breathholds for all methods. Thus, to enable a fair comparison, we also randomly selected 12 breathholds from the STEAM-WET-150 data to give a 60 measurement subset. For clarity, we refer to these subsampled data as "STEAM-WET-60". This subsampling was performed for STEAM-WET-150 data in both healthy volunteers and patients.

Metabolite quantification

Fitted areas for each metabolite A were corrected for T_1 and T_2 decay and proton density according to:

$$S_A^* = S_A \times F_{1,A} \times F_{2,A} \times N_A \tag{3}$$

$$F_{1,A} = \left(1 - e^{-TR/T_{1,A}}\right)^{-1} \tag{4}$$

$$F_{2,A} = e^{TE/T_{2,A}} \tag{5}$$

where S_A refers to the uncorrected signal peak integral, S_A* refers to the corrected signal peak integral, $F_{1,A}$ and $F_{2,A}$ are T_1 and T_2 correction factors and N_A is the proton density.

For the phantom, the T_1 values were determined to be 0.991 s for creatine CH_3 peak and 1.04 s for water, while the T_2 values were determined to be 321 ms for creatine CH_3 peak and 62.7 ms for water. As there are no published values for T_1 and T_2 of cardiac metabolites at 3 T, T_1 and T_2 values from skeletal muscle were used instead. Myocardial lipid T_1 and T_2 values were taken as the average of intramyocellular and extramyocellular lipids. The following T_1 values were used: 0.459 s for the lipid methylene peak;[64] 1.73 s for the creatine CH_3 peak; [49] 1.37 s for choline; [49] and 1.64 s for water. [49] For T_2 correction, the following T_2 values were used: 78 ms for the lipid methylene peak;[64] 177 ms for creatine CH_3 peak; [49] 134 ms for choline; [49] and 35 ms for water.[65]

For in vivo acquisitions, creatine and choline concentrations are calculated in μmol per gram of wet tissue (μmol/g) according to: $[\mathrm{A}] = S_A^* \div S_{water}^* \times [\mathrm{water}]$. The concentration of pure water was taken to be 55.5 mol/L and the myocardial tissue was assumed to contain 72.7% water by weight.[51] Myocardial lipid content is represented by the corrected ratio of the lipid methylene peak (1.28 ppm) area to the unsuppressed water peak area, expressed as a percentage.[3]

Statistical analysis

Sequence performance was assessed by comparing SNR, CRLB and linewidths of the 3 main metabolite peaks: lipid methylene peak, creatine CH_3 peak and choline peak. The values were described using medians and interquartile ranges and paired Wilcoxon signed-rank test (two-tailed) were conducted across all possible pairings for SNR and CRLB in healthy volunteers. Metabolite concentrations in both healthy volunteers and patients were described using means and standard deviations with outliers identified as points more than three scaled median absolute deviations (MAD) away from the median and were excluded from the analysis.

Inter-subject coefficients of variation (σ_i^2) in metabolites were calculated for healthy volunteers by dividing the standard deviation of the metabolite concentrations by the overall mean. Repeatability of STEAM-WET and PRESS-WSC were compared by calculating the intra-subject coefficients of variation (CV) and coefficients of repeatability (CR) for creatine, choline and lipid quantification. The intra-subject coefficient of variation can be calculated by taking the ratio of the standard deviation of within subject measurements (i.e. standard deviation of the difference between measurement 1 and 2, also known as σ_w^2) to the overall mean.[66] The coefficient of repeatability is the value below which the absolute difference of the two measurements would lie with 95% probability and is calculated by multiplying σ_w^2 by 2.77 ($\sqrt{2} \times 1.96$).[67]

Power calculations were also performed using repeatability data from healthy volunteers with G*Power (version 3.1.9.7, Heinrich Heine Universitat, Dusseldorf, Germany).[68,69] The two-tailed a priori power calculation was done with following parameters: Test family: ‘t tests’; Statistical test: ‘Means: Difference between two dependent means (matched pairs)’. In order to calculate the number of subjects needed to determine statistical significance (power = 95%, $\alpha = 0.05$) for a 20% change in concentration for each metabolite for STEAM-WET-150 (150 meas.) and PRESS-WSC (60 meas.), the ‘Mean of difference’ was set to 20% of the mean concentration and ‘SD of difference’ was set to be the standard deviation of within subject measurements (σ_w^2).

Lastly, unpaired Student’s t-tests (two-tailed, equal variance assumed) were conducted to analyse the differences in metabolite concentrations between the healthy volunteers and patients. The metabolite concentrations in healthy volunteers were averaged across both sessions.

Results

Phantom study

The correlation between measured and actual creatine concentration in the phantom for the four sequences is shown in Figure 3. An anomalous point was identified for PRESS-WET and was subsequently excluded. All correlations had $R^2 \geq 0.96$ and the slopes of the linear regression lines (β) ranged between 0.93 and 1.08. The root-mean-squared errors (RMSEs) in concentration measurement for each sequence were: 3.51 mmol/L for PRESS-WET, 7.48 mmol/L for STEAM-WET, 6.15 mmol/L for PRESS-WSC and 6.15 mmol/L for STEAM-WSC. SNR and CRLB values are shown in SI Table 2.

Sequence comparison in healthy volunteers

Figure 4 shows the four spectra acquired from one healthy volunteer: STEAM-WET-150, STEAM-WET-60, STEAM-WSC and PRESS-WSC.

SNR and CRLB values are shown in Figure 5 for healthy volunteers. The metabolite concentrations for all healthy volunteers and patients are presented in Table 1 while SNR, CRLB and linewidths are presented in SI Table 3. The SNR for all three metabolites decreased between STEAM-WET-150 and STEAM-WET-60 with *P*-values of: <0.01 for lipid, 0.03 for creatine, and 0.04 for choline. On the other hand, despite being acquired in less than half the scan time, PRESS-WSC showed no significant decrease in SNR for all peaks compared to STEAM-WET-150. The CRLB values also followed these trends. CRLBs increased (i.e. there was worse fit precision) when the number of measurements was decreased from STEAM-WET-150 to STEAM-WET-60 as expected. Yet with only 60 measurements, the PRESS-WSC sequence gave the lowest CRLB values (best fit precision) for all metabolites.

Lastly, randomisation of the choice of breathholds for STEAM-WET-60 did not have any significant effects on SNR, CRLB or linewidths (SI Figure 4).

Metabolite concentrations in healthy volunteers

Myocardial metabolite concentrations in both healthy volunteers and the patient group are shown in Figure 6. In healthy volunteers, the average fat fraction measured with STEAM-WET-150 was 0.30 ± 0.11% and with PRESS-WSC, it was 0.30 ± 0.15% (*P = 0.78)*; average creatine concentration measured with STEAM-WET-150 was 29.6 ± 7.0 μmol/g with STEAM-WET-150 and with PRESS-WSC, it was 31.5 ± 3.1 μmol/g (*P* = 0.76); and average choline concentration measure with STEAM-WET-150 was 7.9 ± 6.7 μmol/g and with PRESS-WSC, it was 8.3 ± 4.4 μmol/g (*P* = 0.40). There were no significant differences in any of the reported fat fractions and metabolite concentrations between the two sequences.

Repeatability in healthy volunteers

Repeatability results are shown in Table 2 and Bland-Altman plots in Figure 7. For lipid quantification, the coefficients of repeatability (CR) are comparable for both sequences with CR being 0.22 % for STEAM-WET-150 and 0.24 % for PRESS-WSC (60 meas.). For both creatine and choline, PRESS-

WSC showed improved performance. The CR for creatine was 4.19 μmol / g for the PRESS-WSC and 15.1 μmol / g for STEAM-WET-150. A similar improvement was seen for choline, with CR being 1.92 μmol / g for PRESS-WSC and 3.2 μmol / g for STEAM-WET-150.

As an illustration of the power of 3T ^{1}H-MRS to assess creatine and/or choline in clinical studies, Table 3 compares the calculated sample sizes needed to detect a 20% change in metabolite levels for paired and independent studies for both sequences. Sample sizes for independent studies are reported as numbers of participants per group, assuming that only 60% of subjects have quantifiable spectra.

Demonstration in patient cohort

All patients completed the exam. In one patient, the number of measurements per breathhold had to be reduced to 4 to shorten the length of the breathhold. Five patient data sets were discarded as they either had fitted linewidths of less than 2 Hz for any of the metabolites which indicates that there was only noise in the relevant spectral region or a CRLB value for the lipid peak of more than 500% in either of the acquisitions. All five had poor STEAM-WET data, four out of five had also poor PRESS-WSC data.

The remaining eight data sets consisted of seven patients with aortic stenosis with preserved systolic function and one patient suffering from aortic stenosis with impaired systolic function. Figure 8 shows spectra from a patient compared to those from a healthy volunteer.

For the patient cohort, the average fat fractions were 0.48 ± 0.51% when measured with STEAM-WET-150 and 0.25 ± 0.19% when measured with PRESS-WSC, average creatine concentrations were 8.0 ± 2.3 μmol/g when measured with STEAM-WET-150 and 9.3 ± 6.0 μmol/g when measured with PRESS-WSC while average choline concentrations were 4.6 ± 3.2 μmol/g when measured with STEAM-WET-150 and 3.9 ± 3.2 μmol/g when measured with PRESS-WSC. There were no significant differences in the reported fat fraction and metabolite concentrations between the two sequences.

When comparing the patient cohort to healthy volunteers, there were no significant changes in lipid levels for both sequences with $P = 0.26$ for STEAM-WET-150 and $P = 0.94$ for PRESS-WSC, but significant decreases in creatine levels were observed in the patient group compared with healthy volunteers for both sequences ($P = 0.03$ for STEAM-WET-150 and $P < 0.01$ for PRESS-WSC). The average choline levels were also lower in the patient group than in healthy volunteers but these changes were not significant ($P = 0.23$ for STEAM-WET-150 and $P = 0.06$ for PRESS-WSC).

Discussion

Sequence performance

Phantom

Our phantom results show that all four sequences have the potential to quantify creatine levels in the heart in vivo.

Healthy volunteers

For in vivo acquisitions in healthy volunteers, it would have been ideal to compare STEAM-WET, PRESS-WET, STEAM-WSC and PRESS-WSC in a single study with sufficient measurements to get a robust quantitation from all methods. However, due to institutional limits on the duration of a scan, that was not feasible. Thus, PRESS-WET was excluded based on the results of a preliminary study that compared STEAM-WET and PRESS-WET in six healthy volunteers, where it showed inferior SNR, CRLB and linewidths in all three metabolites.

In the main in vivo study, PRESS-WSC showed increased fitting accuracy (i.e. lower CRLB values) and improved repeatability compared to the longer "gold standard" STEAM-WET-150 approach, despite having less than half the number of measurements. These improvements translate to decreases in the number of subjects that would be needed to detect a specified biological effect on creatine or choline metabolism as shown by the power calculations in Table 3. They also indicate that PRESS-WSC may be a shorter (and hence more patient-friendly) alternative to STEAM-WET for cardiac ^{1}H-MRS.

PRESS-WSC also outperformed both STEAM-WET and STEAM-WSC in terms of the raw SNR for matched scan durations. It is tempting to attribute the improvement in SNR seen in PRESS-WSC to the difference in signal intensity between PRESS and STEAM. PRESS acquires a spin-echo signal which inherently has twice the signal intensity compared to a stimulated echo signal acquired by STEAM and this is clearly illustrated in the phantom data set. However, perhaps surprisingly, PRESS-WET showed inferior performance in both SNR and CRLB compared to STEAM-WET in the preliminary in vivo study (SI Figure 3). This indicates that SNR is controlled by other factors in vivo, e.g. differences in sensitivity to motion and diffusion effects between the two SVS sequences.

In terms of linewidths, both WSC sequences showed decreases in metabolite linewidths compared to STEAM-WET-150, which could be due to more accurate frequency and phase corrections based off the larger, narrower residual water peak, rather than a smaller, broader lipid peak. However, the linewidths achieved using STEAM-WSC sequence are on average lower compared to PRESS-WSC. This could be considered surprising as PRESS-WSC was considered superior to STEAM-WSC when assessed with other measures of spectral quality e.g. SNR, CRLB and repeatability. We have observed a similar trend between STEAM-WET and PRESS-WET in our preliminary experiment, thus, we hypothesise that the difference in linewidth could be due to the differences in the STEAM and PRESS sequences. For example, PRESS had a longer TE which would increase sensitivity to small motion effects, and PRESS has 180° pulses that may show more slice edge effects than the 90° pulses in STEAM (with a consequent increase in true voxel size, and hence in linewidth). There are also more complex factors in vivo that might have contributed to the final differences, such as bulk motion and diffusion effects, that will need to be further investigated to fully understand the surprising trend.

Across all in-vivo acquisitions, the bandwidth of water-suppression pulses in WSC was larger (65 Hz or 0.5 ppm) than that for WET (50 Hz or 0.4 ppm). This slightly larger bandwidth was determined through empirical observation in a series of pilot experiments. We suspect that the need for increased water-suppression bandwidth arises because the WSC module needs to either invert or not invert the water. If the water peak drifts in some transients out of the water-suppression bandwidth then this can lead to distorted lineshapes that are not fully cancelled during the WSC post-processing.

This increased water suppression bandwidth means that care should be taken when quantifying metabolites with peaks close to water, e.g. the methylene peak of creatine at 3.9 ppm. It is possible that those peaks might be partially supressed in the presence of severe shot-to-shot frequency drifts. In this study, we only used the peak amplitude of the creatine methyl group at 3.0 ppm for cardiac creatine quantification and not the creatine methylene peak at 3.9 ppm to avoid this potential issue. Furthermore, we note that there is no significant difference in the closer choline signal at 3.2ppm between PRESS-WSC and STEAM-WET in our study, suggesting that this effect is not of concern here.

Another possible factor that affects metabolite quantification is the lack of preparation scans in our protocol. Although preparation scans ensure that a steady-state is reached before signal acquisition, they also lengthen the duration of each breathhold. A quick calculation using literature T_1 values and nominal flip angles shows that the error in quantification due to the slightly higher signal in the first transient is very small, accounting for percentage differences smaller than 0.75 % for $CrCH_3$ and 2.2 % for Cho. These potential errors are modest compared to other sources of error in the fitted amplitudes and can be neglected.

Patient cohort

In the patient cohort, PRESS-WSC also showed comparable fitting accuracy compared to STEAM-WET-150. In just 60 measurements, PRESS-WSC showed an average increase of a mere 2% in CRLB values compared to 150 measurements of STEAM-WET-150 (averaging for lipids, creatine and choline). The benefits of using PRESS-WSC over STEAM-WET become more obvious when comparing PRESS-WSC with STEAM-WET-60 where PRESS-WSC delivered an average decrease of 28% in CRLB values and 18% in linewidths.

STEAM-WET-150 and PRESS-WSC both gave spectra with acceptable quality in all healthy volunteer scans. Yet, in patients STEAM-WET-150 only gave acceptable spectra for quantitative analysis in 8 out of the 13 patients scanned. PRESS-WSC made a small improvement in this respect with one more patient having analysable data quality in spite of the much reduced scan duration. Nevertheless, we are continuing to explore ways to achieve full robustness in patients as well as in healthy volunteers. We believe the underlying issues are not sequence specific but include the familiar issues of heart rate variability, body habitus, compliance with breath holding, age, MR scan familiarity etc.

Repeatability

We showed that in less than half the scan duration (60 vs 150 measurements, or 30 vs 10 breathholds), PRESS-WSC greatly improves intra-subject repeatability for the quantification of creatine and choline, and that it maintains repeatability for lipids (Figure 7) compared to STEAM-WET.

For the repeatability of lipid quantification, Rial *et al.* reported an intra-subject CV of 19% using a STEAM sequence with breathholding at 3T.[3] There have also been a number of previous studies published at 1.5 T using gating methods. Szczepaniak *et al.* reported an intra-subject CV of 19% using a respiratory gating[70] and Felblinger *et al.* reported an intra-subject CV of 13% using a double cardiac and respiratory gating method.[71] Our results for PRESS-WSC in healthy volunteers, i.e. intra-subject CV of 19%, are in good agreement with these reports.

Felblinger *et al.* also reported inter-subject and intra-subject variabilities in cardiac concentrations of creatine and choline (labelled there as "TMA"). In their study, using a double-triggered PRESS sequence at 1.5T, they found the inter-subject/intra-subject variability for creatine to be 16%/10% and for choline to be 56%/9%.[71] Similarly, Nakae *et al.* reported a coefficient of variation of 7.4% in repeated creatine measurements of 8 volunteers using a free breathing PRESS sequence at 1.5T with cardiac gating.[72] These values are similar to ours for PRESS-WSC, however, our STEAM-WET-150 protocol yielded higher inter-subject/intra-subject variability values for both metabolites.

From both the Bland-Altman plots (Figure 7) and the coefficient of repeatability, it can be seen that the lipid repeatability is differently influenced compared to creatine and choline. Possible explanations include that the lipid peak is influenced by J-coupling. The difference in J-coupling evolution with different TEs could account for some of the difference in the repeatability changes. Alternatively, since the heart is surrounded by a layer of epicardial fat, inconsistent diaphragm positions between breathholds and patient motion could perhaps result in some spectral transients being contaminated by epicardial fat.

Simplicity of implementation

We note in passing that many of the prior studies in cardiac creatine and choline quantitation have used relatively complicated motion compensation strategies. Our approach has a benefit that it is straightforward to implement since the only sequence modifications are small alterations to the water suppression module. Other changes are implemented in off-scanner reconstruction tools which are simpler to alter. Therefore, even where our repeatability is comparable to some prior studies, this simplicity of implementation is a pragmatic benefit of the WSC approach.

Metabolite quantification and changes in patient cohort

In both healthy volunteers and patients, the measured fat fractions and metabolite concentrations did not differ significantly between STEAM-WET and PRESS-WSC. Both sequences also gave absolute

myocardial creatine and choline concentrations and fat fractions that were similar to values from the other sequences and to previous studies.[4,6,50,51,71]

There was no significant difference in myocardial lipid concentrations between patients and controls. The results were: 0.30 ± 0.11% in healthy controls and 0.48 ± 0.51% in patients when measured with STEAM-WET-150 ($P = 0.26$); and 0.30 ± 0.15 % in healthy controls and 0.25 ± 0.19% in patients when measured with PRESS-WSC ($P = 0.94$). This was unexpected,[73] however, Marfella et al.[74] reported that lipid contents are significantly higher in aortic stenosis patients with metabolic syndromes than in those without metabolic syndromes. Although none of our patients had diabetes mellitus, insulin resistance is a known correlate of heart failure,[75] so it is likely that our cohort consisted of a mixture of the two groups which would be expected to attenuate differences in observed lipid concentration *vs* healthy volunteers.

There are few reports on myocardial creatine levels in heart disease. For healthy myocardium, Nakae *et al*. reported creatine concentrations measured at 1.5 T to be 27.6 ± 4.1 μmol/g [51] and Bottomley et al. reported 28 ± 6 μmol/g [76]. This is in close agreement with the values we measured in healthy volunteers (29.6 ± 7.0 μmol/g when measured with STEAM-WET-150 and 31.5 ± 3.1 μmol/g when measured with PRESS-WSC). Nakae et al. later studied patients suffering from congestive heart failure due to dilated or hypertrophic cardiomyopathy and found a reduction in myocardial creatine concentrations of 12.5 μmol/g,[50] i.e. a 15.5 μmol/g or 45% reduction. The coefficient of repeatability of creatine concentration measured with our PRESS-WSC (60 meas. over 10 breathholds, CR = 4.19 μmol/g) is roughly one-third this reduction; while that of STEAM-WET-150 (CR = 15.1 μmol/g) is comparable to the reduction, suggesting the PRESS-WSC approach is better suited to assessing creatine depletion. In our patient cohort, we observed a significant decrease in creatine concentrations in patients *vs* volunteers with an average reduction of 21.9 μmol/g across the two sequences. Despite the small cohort scanned in this study, these findings suggest that PRESS-WSC, with its improved repeatability, is a better choice for assessing biologically relevant changes in creatine concentration than STEAM-WET.

In a study conducted at 1.5 T by Gillinder et al., myocardial choline water ratio was 0.24 ± 0.28% before any corrections.[6] By correcting for relaxation and proton density, this result of Gillinder et al. corresponds to a myocardial choline concentration of 9.6 ± 11.1 μmol/g which is in line with our findings of 7.9 ± 6.7 μmol/g with STEAM-WET-150 and 8.3 ± 4.4 μmol/g with PRESS-WSC. Fillmer et al. have also recently quantified "trimethylammonium (TMA)-containing compounds" in the myocardium at 3T, i.e. what we refer to as "choline". They reported a mean TMA to creatine ratio of 0.79 before any corrections.[8] After correcting for relaxation and proton density, the choline to creatine ratio (S_{Cho}^{*}/ S_{Cr}^{*}) reported by them would be 0.21, which again is similar to our results of 0.27 for STEAM-WET-150 and 0.26 for PRESS-WSC.

We compare total choline content in patients with aortic stenosis *vs* volunteers for the first time. The small sample size in the study means that it is impossible to draw any statistically significant conclusions about the variations of total choline between healthy and patient cohorts at this point, but our work demonstrates the feasibility of ^{1}H-MRS as a clinical tool to relate variations in myocardial choline concentration with variations in myocardial performance.

Recently, a number of studies have linked dietary choline intake to cardiovascular diseases in animal models.[77] Human studies to investigate this are more complex due to the significant influence of the intestinal microflora;[78] there is no general agreement yet on the influence of dietary choline intake on the incidence cardiovascular diseases.[79–83] However, preclinical evidence suggests that choline given as an injection has cardio-protective effects in rat models including reducing post-ischemia reperfusion injuries[84] and slowing the progression of hypertension[85] and the whole-blood choline level has been identified as a promising biomarker in acute coronary syndrome.[86,87] However, most of these studies focused on dietary choline intake and/or supplements[79] without measuring any direct changes in choline concentration in the heart. With emerging research aiming to modulate the cholinergic system and thereby target heart disease,[88,89] ^{1}H-MRS is a valuable tool for direct measurement of myocardial choline in vivo.

Future works

In our analysis, we used relaxation times measured in skeletal muscles for quantifying cardiac metabolites. Although a previous imaging study has shown that T_1 and T_2 values for heart and skeletal muscles are very similar at both 1.5T and 3T,[90] we believe that the accuracy in metabolite quantification could be improved by using relaxation values measured directly in the human heart at 3T.

We also noted that the performance gains for PRESS-WSC were more modest in our patient cohort than in volunteers. In a future study, we intend to further optimize the WSC module. E.g. it may be advantageous to simply cycle the water signal by 180° on alternate transients without adding the other water-suppression pulses in what would be a purely "water-cycled" MRS method analogous to "metabolite-cycled" methods. It could also be possible to reduce the spacing between water suppression pulses or to remove the first 90° pulse in the WSC module to make the PRESS-WSC acquisition fit more easily into the shorter diastole seen in high heart-rate, arrhythmic patients like those we scanned in this study.

We have observed decreases in both creatine and choline levels in the patient group when compared to healthy volunteers. However, we only had a limited study size to provide pathophysiology related conclusions. Future studies including more patients with aortic or mitral stenosis are required to gain a better insight into the biochemical changes in the myocardium associated with this diseased state.

Conclusions

We have shown that a water-suppression cycled PRESS sequence improves performance and repeatability in measuring cardiac metabolites (lipids, creatine, choline) relative to the vendor's standard STEAM and PRESS sequences at 3T. We quantified cardiac creatine and choline in a 10-breathhold protocol, which was robust in healthy volunteers. Lastly, in patients with severe symptomatic valvular heart disease listed for clinically indicated valve replacement surgery, we were able to detect changes in cardiac metabolites (creatine, choline, lipids) in a third of the time using PRESS-WSC compared to the vendor's STEAM-WET sequence.

Acknowledgements

BD is currently funded by Gates Cambridge Trust. MAP was supported by a British Heart Foundation Clinical Research Training Fellowship [FS/15/80/31803]. FEM was funded by a UK Medical Research Council Doctoral Training Award (MR/K501256/1), a Scatcherd European Scholarship and the RDM Scholars Programme. OR is supported by a British Heart Foundation Intermediate Fellowship. LV acknowledges support of the Slovak Grant Agencies VEGA [2/0003/20] and APVV [#19-0032]. CTR is funded by a Sir Henry Dale Fellowship from the Wellcome Trust and the Royal Society [098436/Z/12/B].

We acknowledge support from the Oxford NIHR BRC, and the Cambridge NIHR BRC. The views expressed are those of the author(s) and not necessarily those of the NHS, the NIHR or the Department of Health and Social Care.

Data availability statement

Data available on request due to privacy/ethical restrictions.

References

1. Goldberg IJ, Trent CM, Schulze PC. Lipid metabolism and toxicity in the heart. *Cell Metab*. 2012;15(6):805-812. doi:10.1016/j.cmet.2012.04.006

2. Boudina S, Abel ED. Diabetic cardiomyopathy revisited. *Circulation*. 2007;115(25):3213-3223. doi:10.1161/CIRCULATIONAHA.106.679597

3. Rial B, Robson MD, Neubauer S, Schneider JE. Rapid quantification of myocardial lipid content in humans using single breath-hold 1H MRS at 3 Tesla. *Magn Reson Med*. 2011;66(3):619-624. doi:10.1002/mrm.23011

4. Faller KME, Lygate CA, Neubauer S, Schneider JE. (1)H-MR spectroscopy for analysis of cardiac lipid and creatine metabolism. *Heart Fail Rev*. 2013;18(5):657-668. doi:10.1007/s10741-012-9341-z

5. Gastl M, Peereboom SM, Gotschy A, et al. Myocardial triglycerides in cardiac amyloidosis assessed by proton cardiovascular magnetic resonance spectroscopy. *J Cardiovasc Magn Reson*. 2019;21(1):10. doi:10.1186/s12968-019-0519-6

6. Gillinder L, Goo SY, Cowin G, et al. Quantification of Intramyocardial Metabolites by Proton Magnetic Resonance Spectroscopy. *Front Cardiovasc Med*. 2015;2:24.

doi:10.3389/fcvm.2015.00024

7. Peereboom SM, Gastl M, Fuetterer M, Kozerke S. Navigator-free metabolite-cycled proton spectroscopy of the heart. *Magn Reson Med*. 2020;83(3):795-805. doi:10.1002/mrm.27961

8. Fillmer A, Hock A, Cameron D, Henning A. Non-Water-Suppressed1H MR Spectroscopy with Orientational Prior Knowledge Shows Potential for Separating Intra- and Extramyocellular Lipid Signals in Human Myocardium. *Sci Rep*. 2017;7(1):16898. doi:10.1038/s41598-017-16318-0

9. Neubauer S. The Failing Heart — An Engine Out of Fuel. *N Engl J Med*. 2007;356(11):1140-1151. doi:10.1056/NEJMra063052

10. Weiss K, Bottomley PA, Weiss RG. On the theoretical limits of detecting cyclic changes in cardiac high-energy phosphates and creatine kinase reaction kinetics using in vivo ^{31}P MRS. *NMR Biomed*. 2015;28(6):694-705. doi:10.1002/nbm.3302

11. Bottomley PA. MRS Studies of Creatine Kinase Metabolism in Human Heart. In: *EMagRes*. Chichester, UK: John Wiley & Sons, Ltd; 2016:1183-1202. doi:10.1002/9780470034590.emrstm1488

12. Ingwall JS, Weiss RG. Is the failing heart energy starved? On using chemical energy to support cardiac function. *Circ Res*. 2004;95(2):135-145. doi:10.1161/01.RES.0000137170.41939.d9

13. Ingwall JS, Kramer MF, Fifer MA, et al. The Creatine Kinase System in Normal and Diseased Human Myocardium. *N Engl J Med*. 1985;313(17):1050-1054. doi:10.1056/NEJM198510243131704

14. Bottomley PA. NMR Spectroscopy of the Human Heart. In: Grant DM, Harris RK, eds. *Encyclopedia of Nuclear Magnetic Resonance, Volume 1: Historical Perspectives*. Chichester, UK: Wiley; 2007. doi:10.1002/9780470034590.emrstm0345

15. Bottomley PA, Weiss RG. Noninvasive Localized MR Quantification of Creatine Kinase Metabolites in Normal and Infarcted Canine Myocardium. *Radiology*. 2001;219(2):411-418. doi:10.1148/radiology.219.2.r01ma39411

16. Valkovič L, Clarke WT, Schmid AI, et al. Measuring inorganic phosphate and intracellular pH in the healthy and hypertrophic cardiomyopathy hearts by in vivo 7T 31P-cardiovascular magnetic resonance spectroscopy. *J Cardiovasc Magn Reson*. 2019;21(1):19. doi:10.1186/s12968-019-0529-4

17. Tian R, Ingwall JS. Energetic basis for reduced contractile reserve in isolated rat hearts. *Am J Physiol - Hear Circ Physiol*. 1996;270(4 39-4). doi:10.1152/ajpheart.1996.270.4.h1207

18. Gabr RE, El-Sharkawy A-MM, Schär M, et al. Cardiac work is related to creatine kinase energy supply in human heart failure: a cardiovascular magnetic resonance spectroscopy study. *J Cardiovasc Magn Reson*. 2018;20(1):81. doi:10.1186/s12968-018-0491-6

19. Martin C, Schulz R, Rose J, Heusch G. Inorganic phosphate content and free energy change of ATP hydrolysis in regional short-term hibernating myocardium. *Cardiovasc Res*. 1998;39(2):318-326. doi:10.1016/S0008-6363(98)00086-8

20. Schwarzer M, Faerber G, Rueckauer T, et al. The metabolic modulators, Etomoxir and NVP-LAB121, fail to reverse pressure overload induced heart failure in vivo. *Basic Res Cardiol*. 2009;104(5):547-557. doi:10.1007/s00395-009-0015-5

21. Lionetti V, Stanley WC, Recchia FA. Modulating fatty acid oxidation in heart failure. *Cardiovasc Res*. 2011;90(2):202-209. doi:10.1093/cvr/cvr038

22. Zeisel SH, da Costa K-AA. Choline: an essential nutrient for public health. *Nutr Rev*. 2009;67(11):615-623. doi:10.1111/j.1753-4887.2009.00246.x

23. Gordan R, Gwathmey JK, Xie L-H. Autonomic and endocrine control of cardiovascular function. *World J Cardiol*. 2015;7(4):204. doi:10.4330/wjc.v7.i4.204

24. Mufson EJ, Counts SE, Perez SE, Ginsberg SD. Cholinergic system during the progression of Alzheimer's disease: Therapeutic implications. *Expert Rev Neurother*. 2008;8(11):1703-1718. doi:10.1586/14737175.8.11.1703

25. Howe FA, Opstad KS. 1H MR spectroscopy of brain tumours and masses. *NMR Biomed*. 2003;16(3):123-131. doi:10.1002/nbm.822

26. Bartella L, Huang W. Proton (^{1} H) MR Spectroscopy of the Breast. *RadioGraphics*. 2007;27(suppl_1):S241-S252. doi:10.1148/rg.27si075504

27. Zhang L, Zhao X, Ouyang H, Wang S, Zhou C. Diagnostic value of 3.0T (1)H MRS with choline-containing compounds ratio (ΔCCC) in primary malignant hepatic tumors. *Cancer Imaging*. 2016;16(1):25. doi:10.1186/s40644-016-0082-4

28. Helms G, Piringer A. Restoration of motion-related signal loss and line-shape deterioration of proton MR spectra using the residual water as intrinsic reference. *Magn Reson Med*. 2001;46(2):395-400. doi:10.1002/mrm.1203

29. Shetty AN, Gabr RE, Rendon DA, Cassady CI, Mehollin-Ray AR, Lee W. Improving spectral quality in fetal brain magnetic resonance spectroscopy using constructive averaging. *Prenat Diagn*. 2015;35(13):1294-1300. doi:10.1002/pd.4689

30. Bolan PJ, Henry P-G, Baker EH, Meisamy S, Garwood M. Measurement and correction of respiration-inducedB0 variations in breast1H MRS at 4 Tesla. *Magn Reson Med*. 2004;52(6):1239-1245. doi:10.1002/mrm.20277

31. Gabr RE, Sathyanarayana S, Schär M, Weiss RG, Bottomley PA. On restoring motion-induced signal loss in single-voxel magnetic resonance spectra. *Magn Reson Med*. 2006;56(4):754-760. doi:10.1002/mrm.21015

32. Star-Lack JM, Adalsteinsson E, Gold GE, Ikeda DM, Spielman DM. Motion correction and lipid suppression for 1H magnetic resonance spectroscopy. *Magn Reson Med*. 2000;43(3):325-330. doi:10.1002/(SICI)1522-2594(200003)43:3<325::AID-MRM1>3.0.CO;2-8

33. Near J, Edden R, Evans CJ, El Paquin R, Harris A, Jezzard P. Frequency and Phase Drift Correction of Magnetic Resonance Spectroscopy Data by Spectral Registration in the Time Domain. doi:10.1002/mrm.25094

34. Ernst T, Li J. A novel phase and frequency navigator for proton magnetic resonance spectroscopy using water-suppression cycling. *Magn Reson Med*. 2011;65(1):13-17. doi:10.1002/mrm.22582

35. Dreher W, Leibfritz D. New method for the simultaneous detection of metabolites and water in localized in vivo1H nuclear magnetic resonance spectroscopy. *Magn Reson Med*. 2005;54(1):190-195. doi:10.1002/mrm.20549

36. Baumgartner H, Hung J, Bermejo J, et al. Recommendations on the echocardiographic assessment of aortic valve stenosis: A focused update from the European Association of Cardiovascular Imaging and the American Society of Echocardiography. *Eur Heart J Cardiovasc Imaging*. 2017;18(3):254-275. doi:10.1093/ehjci/jew335

37. Iung B, Baron G, Butchart EG, et al. A prospective survey of patients with valvular heart disease in Europe: The Euro Heart Survey on valvular heart disease. *Eur Heart J*. 2003;24(13):1231-1243. doi:10.1016/S0195-668X(03)00201-X

38. Dahl JS, Eleid MF, Michelena HI, et al. Effect of left ventricular ejection fraction on postoperative outcome in patients with severe aortic stenosis undergoing aortic valve

replacement. *Circ Cardiovasc Imaging*. 2015;8(4). doi:10.1161/CIRCIMAGING.114.002917

39. Ito S, Miranda WR, Nkomo VT, et al. Reduced Left Ventricular Ejection Fraction in Patients With Aortic Stenosis. *J Am Coll Cardiol*. 2018;71(12):1313-1321. doi:10.1016/j.jacc.2018.01.045

40. Bohbot Y, de Meester de Ravenstein C, Chadha G, et al. Relationship Between Left Ventricular Ejection Fraction and Mortality in Asymptomatic and Minimally Symptomatic Patients With Severe Aortic Stenosis. *JACC Cardiovasc Imaging*. 2019;12(1):38-48. doi:10.1016/j.jcmg.2018.07.029

41. Peterzan MA, Lygate CA, Neubauer S, Rider OJ. Metabolic remodeling in hypertrophied and failing myocardium: A review. *Am J Physiol - Hear Circ Physiol*. 2017;313(3):H597-H616. doi:10.1152/ajpheart.00731.2016

42. Peterzan MA, Lewis AJM, Neubauer S, Rider OJ. Non-invasive investigation of myocardial energetics in cardiac disease using 31P magnetic resonance spectroscopy. *Cardiovasc Diagn Ther*. 2020;10(3):625-635. doi:10.21037/cdt-20-275

43. Peterzan MA, Clarke WT, Lygate CA, et al. Cardiac Energetics in Patients With Aortic Stenosis and Preserved Versus Reduced Ejection Fraction. *Circulation*. 2020;141(24):1971-1985. doi:10.1161/CIRCULATIONAHA.119.043450

44. Bache RJ, Zhang J, Path G, et al. High-energy phosphate responses to tachycardia and inotropic stimulation in left ventricular hypertrophy. *Am J Physiol - Hear Circ Physiol*. 1994;266(5 35-5). doi:10.1152/ajpheart.1994.266.5.h1959

45. Lygate CA, Fischer A, Sebag-Montefiore L, Wallis J, ten Hove M, Neubauer S. The creatine kinase energy transport system in the failing mouse heart. *J Mol Cell Cardiol*. 2007;42(6):1129-1136. doi:10.1016/j.yjmcc.2007.03.899

46. Ye Y, Wang C, Zhang J, et al. Myocardial creatine kinase kinetics and isoform expression in hearts with severe LV hypertrophy. *Am J Physiol - Hear Circ Physiol*. 2001;281(1 50-1). doi:10.1152/ajpheart.2001.281.1.h376

47. Tian R, Nascimben L, Ingwall JS, Lorell BH. Failure to Maintain a Low ADP Concentration Impairs Diastolic Function in Hypertrophied Rat Hearts. *Circulation*. 1997;96(4):1313-1319. doi:10.1161/01.CIR.96.4.1313

48. Ogg RJ, Kingsley PB, Taylor JS. WET, a T1- and B1-Insensitive Water-Suppression Method for in Vivo Localized 1H NMR Spectroscopy. *J Magn Reson Ser B*. 1994;104(1):1-10. doi:10.1006/jmrb.1994.1048

49. Thomson LEJ, Kim RJ, Judd RM. Magnetic resonance imaging for the assessment of myocardial viability. *J Magn Reson Imaging*. 2004;19(6):771-788. doi:10.1002/jmri.20075

50. Nakae I, Mitsunami K, Matsuo S, et al. Assessment of Myocardial Creatine Concentration in Dysfunctional Human Heart by Proton Magnetic Resonance Spectroscopy. *Magn Reson Med Sci*. 2004;3(1):19-25. doi:10.2463/mrms.3.19

51. Nakae I, Mitsunami K, Omura T, et al. Proton magnetic resonance spectroscopy can detect creatine depletion associated with the progression of heart failure in cardiomyopathy. *J Am Coll Cardiol*. 2003;42(9):1587-1593. doi:10.1016/J.JACC.2003.05.005

52. Weiss K, Martini N, Boesiger P, Kozerke S. Cardiac proton spectroscopy using large coil arrays. *NMR Biomed*. 2013;26(3):276-284. doi:10.1002/nbm.2845

53. Liu C-Y, Redheuil A, Ouwerkerk R, Lima JAC, Bluemke DA. Myocardial fat quantification in humans: Evaluation by two-point water-fat imaging and localized proton spectroscopy. *Magn Reson Med*. 2010;63(4):892-901. doi:10.1002/mrm.22289

54. Kankaanpää M, Lehto H-R, Pärkkä JP, et al. Myocardial Triglyceride Content and Epicardial Fat Mass in Human Obesity: Relationship to Left Ventricular Function and Serum Free Fatty Acid Levels. *J Clin Endocrinol Metab*. 2006;91(11):4689-4695. doi:10.1210/jc.2006-0584

55. Petritsch B, Köstler H, Weng AM, et al. Myocardial lipid content in Fabry disease: a combined 1H-MR spectroscopy and MR imaging study at 3 Tesla. *BMC Cardiovasc Disord*. 2016;16(1):205. doi:10.1186/s12872-016-0382-4

56. Schär M, Kozerke S, Boesiger P. Navigator gating and volume tracking for double-triggered cardiac proton spectroscopy at 3 Tesla. *Magn Reson Med*. 2004;51(6):1091-1095. doi:10.1002/mrm.20123

57. Rial B. Development of Proton Magnetic Resonance Spectroscopy in Human Heart at 3 Tesla. 2010.

58. Rodgers CT, Robson MD. Coil combination for receive array spectroscopy: Are data-driven methods superior to methods using computed field maps? *Magn Reson Med*. 2016;75(2):473-487. doi:10.1002/mrm.25618

59. Purvis LAB, Clarke WT, Biasiolli L, Valkovič L, Robson MD, Rodgers CT. OXSA: An open-source magnetic resonance spectroscopy analysis toolbox in MATLAB. Motta A, ed. *PLoS One*. 2017;12(9):e0185356. doi:10.1371/journal.pone.0185356

60. Pijnappel WW., van den Boogaart A, de Beer R, van Ormondt D. SVD-based quantification of magnetic resonance signals. *J Magn Reson*. 1992;97(1):122-134. doi:10.1016/0022-2364(92)90241-X

61. Vanhamme, Fierro, Van Huffel S, de Beer R. Fast Removal of Residual Water in Proton Spectra. *J Magn Reson*. 1998;132(2):197-203. http://www.ncbi.nlm.nih.gov/pubmed/9632545. Accessed January 30, 2019.

62. Ernst RR, Bodenhausen G, Wokaun A. *Principles of Nuclear Magnetic Resonance in One and Two Dimensions*. Clarendon Press; 1987. https://books.google.com.sg/books?id=XndTnwEACAAJ.

63. Cavassila S, Deval S, Huegen C, van Ormondt D, Graveron-Demilly D. Cramér-Rao bounds: an evaluation tool for quantitation. *NMR Biomed*. 2001;14(4):278-283. doi:10.1002/nbm.701

64. Wang L, Salibi N, Wu Y, Schweitzer ME, Regatte RR. Relaxation Times of Skeletal Muscle Metabolites at 7T. *J Magn Reson Imaging*. 2009;29:1457-1464. doi:10.1002/jmri.21776

65. Wang X, Salibi N, Fayad LM, Barker PB. Proton magnetic resonance spectroscopy of skeletal muscle: a comparison of two quantitation techniques. *J Magn Reson*. 2014;243:81-84. doi:10.1016/j.jmr.2014.03.010

66. Reinstein DZ, Archer TJ, Silverman RH, Coleman DJ. Accuracy, repeatability, and reproducibility of Artemis very high-frequency digital ultrasound arc-scan lateral dimension measurements. *J Cataract Refract Surg*. 2006;32(11):1799-1802. doi:10.1016/j.jcrs.2006.07.017

67. Bartlett JW, Frost C. Reliability, repeatability and reproducibility: analysis of measurement errors in continuous variables. *Ultrasound Obstet Gynecol*. 2008;31(4):466-475. doi:10.1002/uog.5256

68. Faul F, Erdfelder E, Lang AG, Buchner A. G*Power 3: A flexible statistical power analysis program for the social, behavioral, and biomedical sciences. In: *Behavior Research Methods*. Vol 39. Psychonomic Society Inc.; 2007:175-191. doi:10.3758/BF03193146

69. Erdfelder E, FAul F, Buchner A, Lang AG. Statistical power analyses using G*Power 3.1: Tests for correlation and regression analyses. *Behav Res Methods*. 2009;41(4):1149-1160.

doi:10.3758/BRM.41.4.1149

70. Szczepaniak LS, Dobbins RL, Metzger GJ, et al. Myocardial triglycerides and systolic function in humans: In vivo evaluation by localized proton spectroscopy and cardiac imaging. *Magn Reson Med*. 2003;49(3):417-423. doi:10.1002/mrm.10372

71. Felblinger J, Jung B, Slotboom J, Boesch C, Kreis R. Methods and reproducibility of cardiac/respiratory double-triggered1H-MR spectroscopy of the human heart. *Magn Reson Med*. 1999;42(5):903-910. doi:10.1002/(SICI)1522-2594(199911)42:5<903::AID-MRM10>3.0.CO;2-N

72. Nakae I, Mitsunami K, Matsuo S, et al. Myocardial Creatine Concentration in Various Nonischemic Heart Diseases Assessed by 1H Magnetic Resonance Spectroscopy. *Circ J*. 2005;69(6):711-716. doi:10.1253/circj.69.711

73. Mahmod M, Bull S, Suttie JJ, et al. Myocardial Steatosis and Left Ventricular Contractile Dysfunction in Patients With Severe Aortic Stenosis. *Circ Cardiovasc Imaging*. 2013;6(5):808-816. doi:10.1161/CIRCIMAGING.113.000559

74. Marfella R, Di Filippo C, Portoghese M, et al. Myocardial lipid accumulation in patients with pressure-overloaded heart and metabolic syndrome. *J Lipid Res*. 2009;50(11):2314-2323. doi:10.1194/jlr.P900032-JLR200

75. Witteles RM, Fowler MB. Insulin-Resistant Cardiomyopathy: Clinical Evidence, Mechanisms, and Treatment Options. *J Am Coll Cardiol*. 2008;51(2):93-102. doi:10.1016/J.JACC.2007.10.021

76. Bottomley PA, Weiss RG. Non-invasive magnetic-resonance detection of creatine depletion in non-viable infarcted myocardium. *Lancet*. 1998;351(9104):714-718. doi:10.1016/S0140-6736(97)06402-7

77. Organ CL, Otsuka H, Bhushan S, et al. Choline diet and its gut microbe-derived metabolite, trimethylamine N-oxide, exacerbate pressure overload-induced heart failure. *Circ Hear Fail*. 2016;9(1). doi:10.1161/CIRCHEARTFAILURE.115.002314

78. Wang Z, Klipfell E, Bennett BJ, et al. Gut flora metabolism of phosphatidylcholine promotes cardiovascular disease. *Nature*. 2011;472(7341):57-63. doi:10.1038/nature09922

79. Meyer KA, Shea JW. Dietary choline and betaine and risk of cvd: A systematic review and meta-analysis of prospective studies. *Nutrients*. 2017;9(7):711. doi:10.3390/nu9070711

80. Bidulescu A, Chambless LE, Siega-Riz AM, Zeisel SH, Heiss G. Usual choline and betaine dietary intake and incident coronary heart disease: The Atherosclerosis Risk in Communities (ARIC) Study. *BMC Cardiovasc Disord*. 2007;7. doi:10.1186/1471-2261-7-20

81. Rajaie S, Esmaillzadeh A. Dietary choline and betaine intakes and risk of cardiovascular diseases: review of epidemiological evidence. *ARYA Atheroscler*. 2011;7(2):78-86. http://www.ncbi.nlm.nih.gov/pubmed/22577451. Accessed January 25, 2019.

82. Zhu W, Wang Z, Tang WHW, Hazen SL. Gut microbe-generated trimethylamine N-oxide from dietary choline is prothrombotic in subjects. *Circulation*. 2017;135(17):1671-1673. doi:10.1161/circulationaha.116.025338

83. Millard HR, Musani SK, Dibaba DT, et al. Dietary choline and betaine; associations with subclinical markers of cardiovascular disease risk and incidence of CVD, coronary heart disease and stroke: the Jackson Heart Study. *Eur J Nutr*. 2018;57(1):51-60. doi:10.1007/s00394-016-1296-8

84. Hang P, Zhao J, Su Z, et al. Choline Inhibits Ischemia-Reperfusion-Induced Cardiomyocyte Autophagy in Rat Myocardium by Activating Akt/mTOR Signaling. *Cell Physiol Biochem*.

2018;45(5):2136-2144. doi:10.1159/000488049

85. Liu L, Lu Y, Bi X, et al. Choline ameliorates cardiovascular damage by improving vagal activity and inhibiting the inflammatory response in spontaneously hypertensive rats. *Sci Rep*. 2017;7(1):42553. doi:10.1038/srep42553

86. Danne O, Möckel M. Choline in acute coronary syndrome: an emerging biomarker with implications for the integrated assessment of plaque vulnerability. *Expert Rev Mol Diagn*. 2010;10(2):159-171. doi:10.1586/erm.10.2

87. Apple FS, Wu AHA, Mair J, et al. Future biomarkers for detection of ischemia and risk stratification in acute coronary syndrome. *Clin Chem*. 2005;51(5):810-824. doi:10.1373/clinchem.2004.046292

88. Roy A, Guatimosim S, Prado VF, Gros R, Prado MAM. Cholinergic activity as a new target in diseases of the heart. *Mol Med*. 2015;20(1):527-537. doi:10.2119/molmed.2014.00125

89. Saw EL, Kakinuma Y, Fronius M, Katare R. The non-neuronal cholinergic system in the heart: A comprehensive review. *J Mol Cell Cardiol*. 2018;125:129-139. doi:10.1016/J.YJMCC.2018.10.013

90. Stanisz GJ, Odrobina EE, Pun J, et al. T1, T2 relaxation and magnetization transfer in tissue at 3T. *Magn Reson Med*. 2005;54(3):507-512. doi:10.1002/mrm.20605

Figures

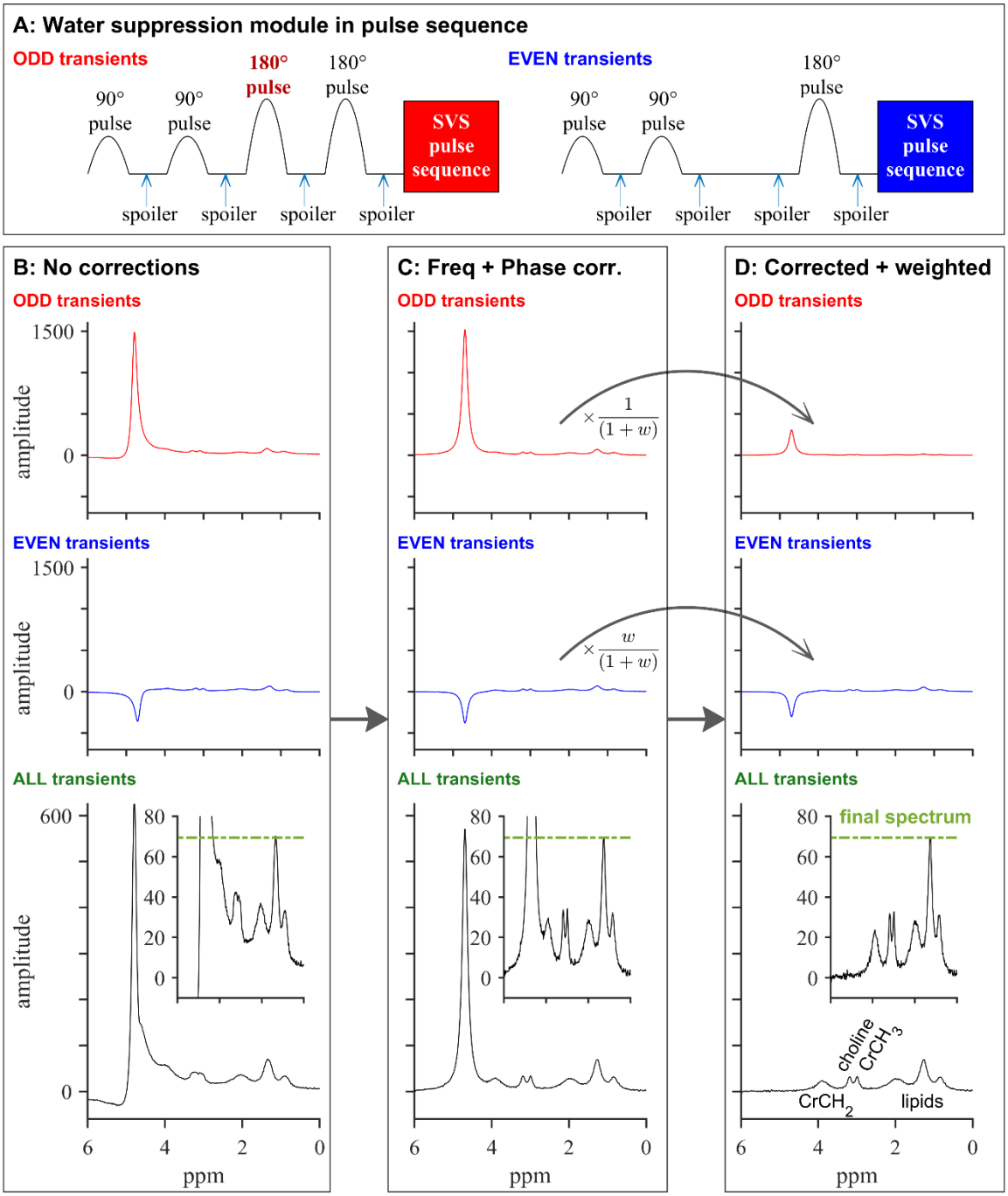

Figure 1: Explanation of the water-suppression cycling 1H-MRS approach. (A) Simplified pulse diagram showing the difference in water-suppression between odd and even numbered transients. (B) Top: Frequency domain plots of simulated example odd and even transients. Bottom: Average of these. Inset: zoom to show metabolite signal amplitudes. (C) Equivalent plots after per-transient frequency and phase correction based on the residual water peak. (D) Equivalent plots with per-transient frequency and phase correction and weighting according to Eq. 2. The final WSC spectrum is shown at the bottom right. Note that a green dashed line is plotted at the same vertical position in all three columns to illustrate that the WSC processing preserves metabolite peak amplitudes.

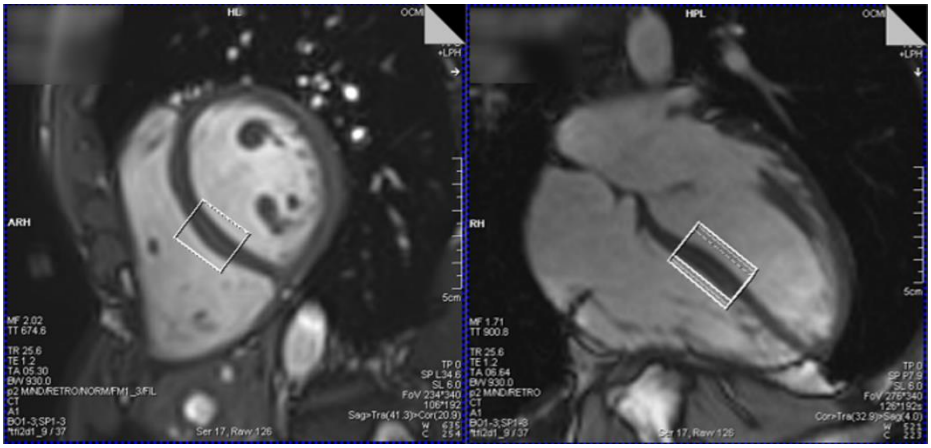

Figure 2: Voxel position (white box) as shown on a short-axis view (left) and a horizontal long axis view (right).

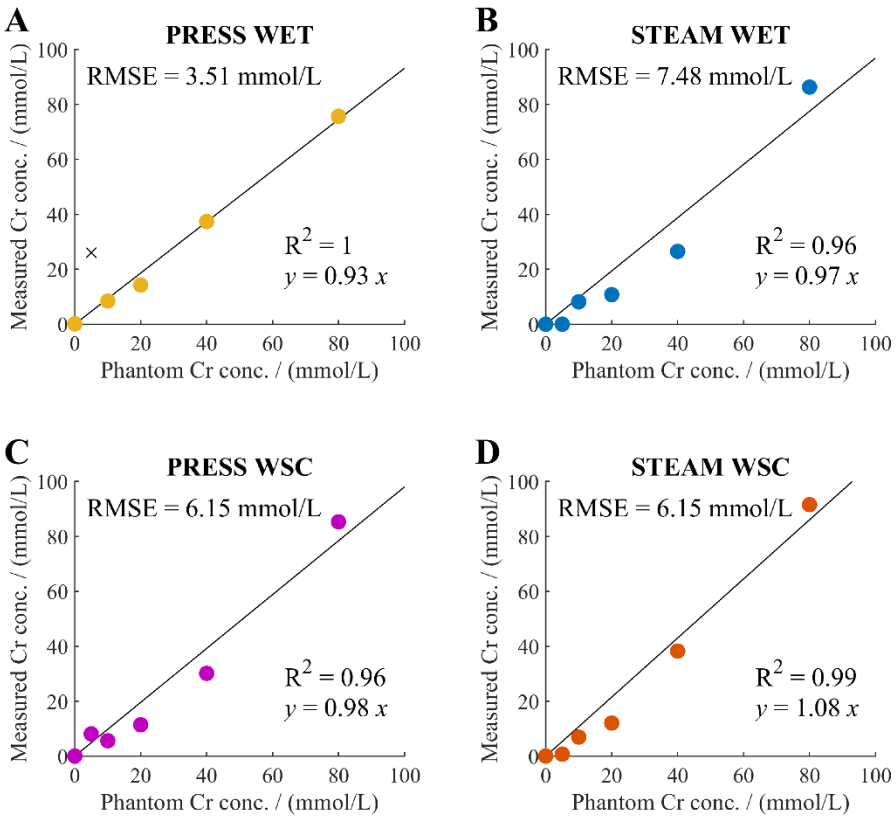

Figure 3: Correlation of measured creatine concentration and the actual creatine concentration in each phantom compartment measured with A) PRESS-WSC; B) STEAM-WET; C) PRESS-WSC; and D) STEAM-WSC. An anomalous point in panel (A) has been identified and labelled using a black cross. This point was subsequently excluded from data analysis.

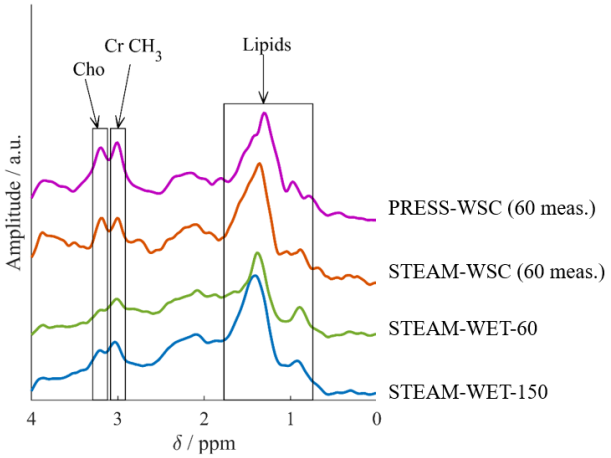

Figure 4: Spectra from a single volunteer comparing all four protocols tested in the volunteer study.

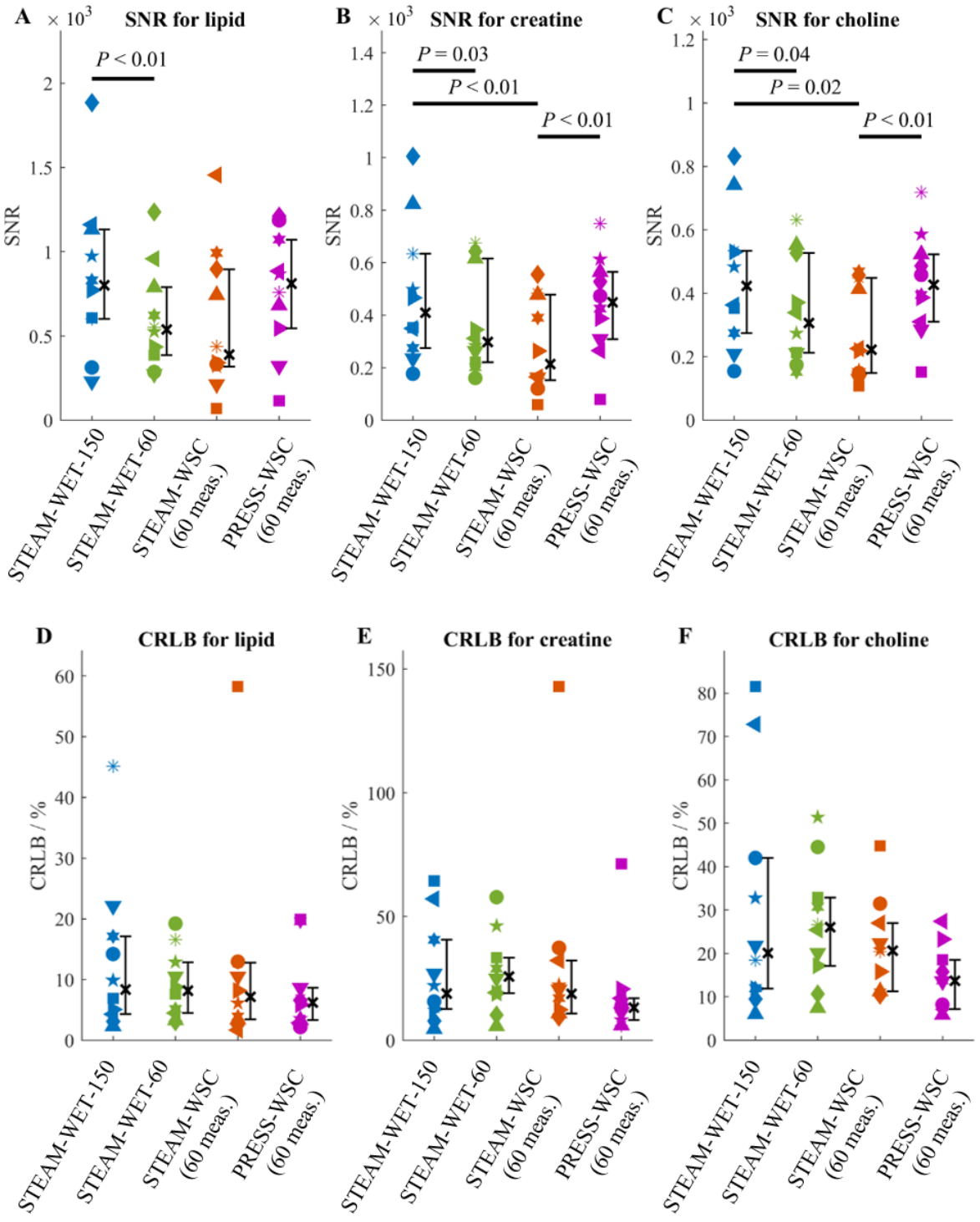

Figure 5: Comparision of CRLB and SNR across all four protocols tested in the volunteer study for lipids (A,D), creatine (B,E) and choline (C,F).The black cross and the attached whiskers represent the median and the interquartile across all healthy volunteers. For each plot, Wilcoxon signed-rank test were conducted across all 6 possible pairs and all significant p values ($p \leqslant 0.05$) are shown.

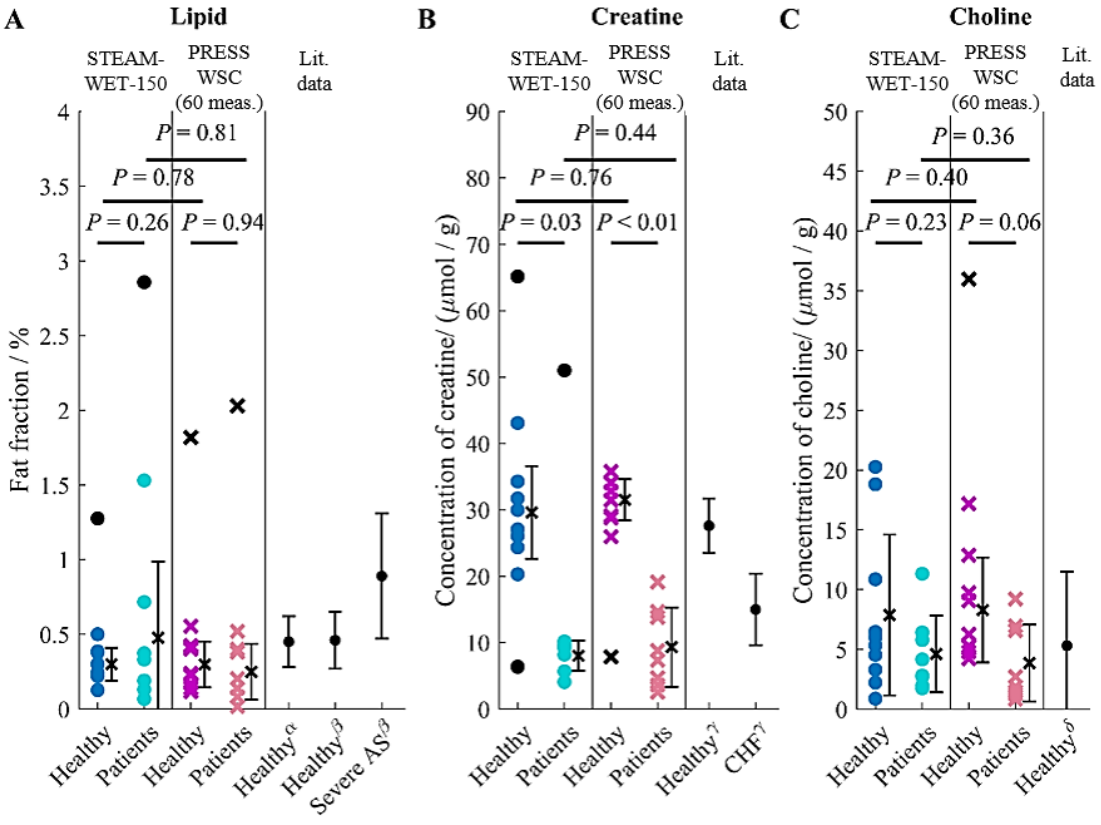

Figure 6: Comparison of metabolite concentrations and fat fractions in healthy and patient cohort with STEAM-WET-150 ('o') and PRESS-WSC ('×') for A) lipids, B) creatine, C) choline against various published literature values. For healthy volunteers, the values are an average between scan 1 and scan 2 while literature data are taken from the following sources: Rial et al. 2011(α)[3], Mahmod et al. 2013 (β)[73], Nakae et al. 2004 (γ)[50] and Gilinder et al. 2015 (δ)[6]. Data from Rial et al. 2011 and Mahmod et al. were obtained 3 T, while Nakae et al. and Gilinder et al. obtained their data at 1.5 T. For our study, data points more than 1.5 interquartile ranges above the upper quartile or below the lower quartile are treated as outliers (denoted in black). The black cross and the attached whiskers represent the mean and the standard deviations across all healthy volunteers. The P values from the unpaired Student's t-tests are also provided. The following acronyms are also used: severe AS = severe aortic stenosis; CHF = chronic heart failure.

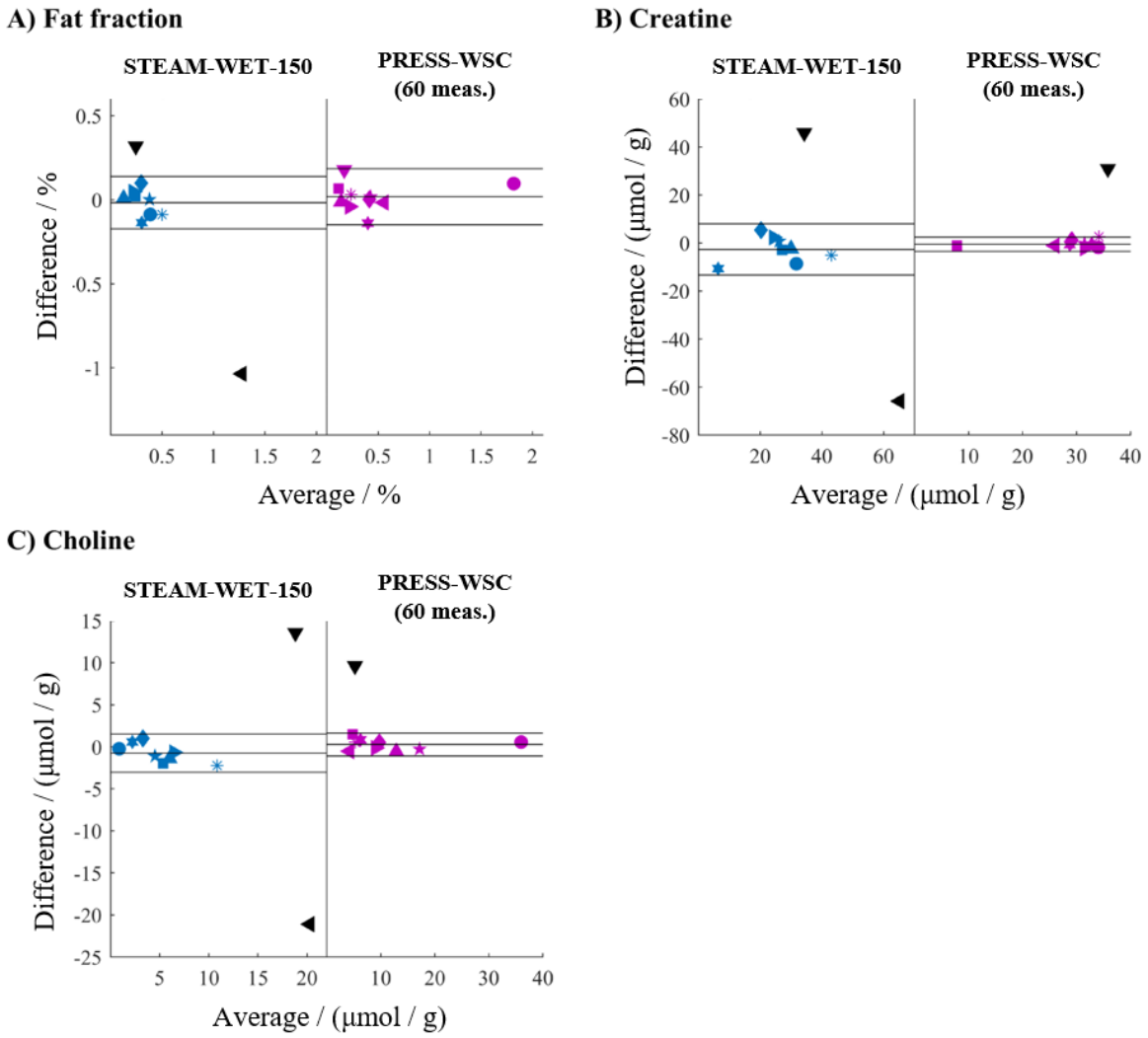

Figure 7: Bland-Altmann plots: A) for lipids with STEAM-WET-150 (coefficient of repeatability (CR) = 0.22%) and PRESS-WSC (CR = 0.24%); B) for creatine with STEAM-WET-150 (CR = 15.1 µmol / g) and PRESS-WSC (CR = 4.19 µmol / g); and C) for choline with STEAM-WET-150 (CR = 3.2 µmol / g) and PRESS-WSC (CR = 1.92 µmol / g). The mean difference and the limits of agreement are shown. Data points more than 1.5 interquartile ranges above the upper quartile or below the lower quartile are treated as outliers (coloured black).

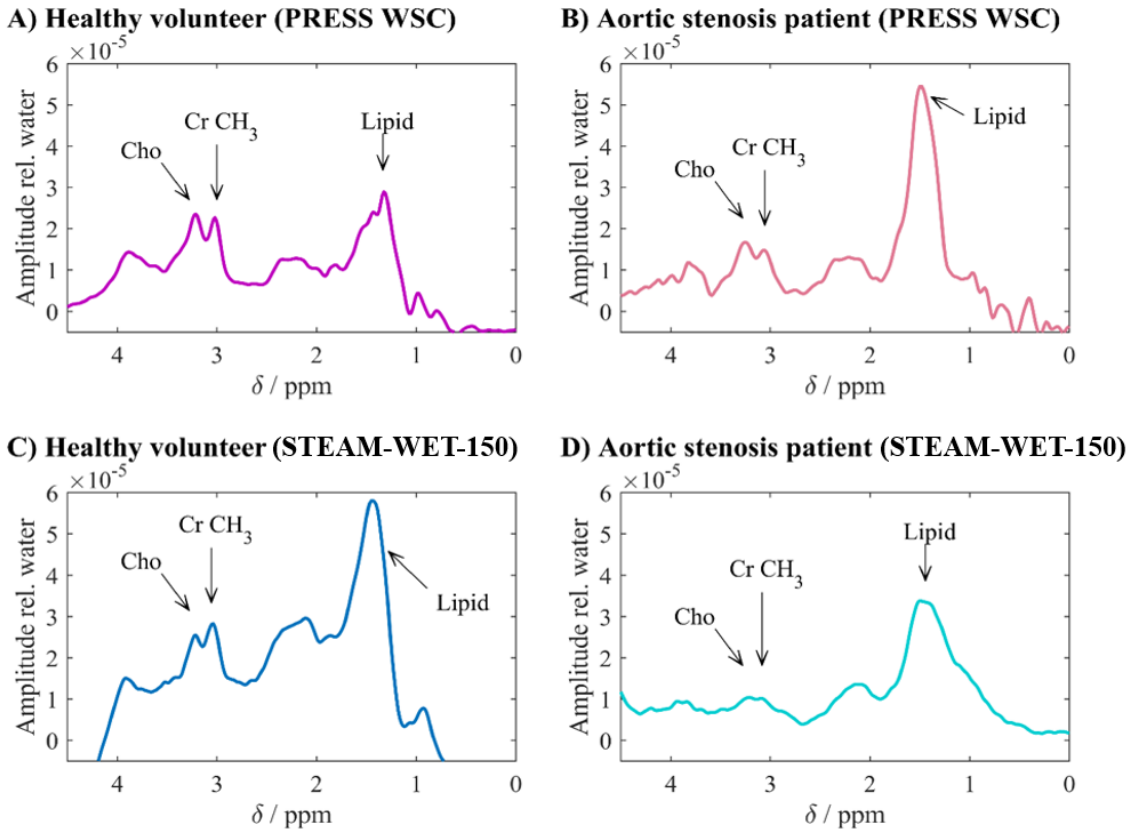

Figure 8: Spectra from a healthy volunteer (left, both A and C) compared to that of a patient (right, both B and D) suffering from aortic stenosis. The spectra are acquired with PRESS-WSC in a healthy volunteer (A) and a patient (B), and with STEAM-WET-150 in a healthy volunteer (C) and a patient (D). All spectra are scaled by the corresponding water peak amplitude. A decrease in creatine is seen between these pairs.

Tables

*Table 1: Metabolite concentrations and fat fractions (mean ± SD over all n subjects) are shown in (A), with the number of outliers in each data set denoted by the number of '$^{+}$' in brackets, i.e. ($^{+}$) means one outlier, ($^{++}$) means two outliers etc. Any statistically significant changes in metabolite concentration between healthy volunteers and patients as measured by a particular sequence is indicated by * (when P < 0.05) or ** (when P<0.01).*

A) Mean ± standard deviation of metabolite concentration					
Group	Sequence	Meas.	Lipid (%)	Creatine (μmol/g)	Choline (μmol/g)
Healthy n = 10	STEAM-WET-150	150	0.30 ± 0.15 ($^{+}$)	29.6 ± 7.0 ($^{++}$) *	7.9 ± 6.7
	PRESS-WSC	60	0.30 ± 0.11 ($^{+}$)	31.5 ± 3.1 ($^{+}$) **	8.3 ± 4.4 ($^{+}$) *
Patients n = 8	STEAM-WET-150	150	0.48 ± 0.51 ($^{+}$)	8.0 ± 2.3 ($^{+}$) *	4.6 ± 3.2
	PRESS-WSC	60	0.25 ± 0.19 ($^{+}$)	9.3 ± 6.0 **	3.9 ± 3.2 *

Table 2: Inter-subject coefficient of variation (σ_i^2), intra-subject coefficient of variation (σ_w^2) and coefficient of repeatability for lipids, creatine and choline quantification in healthy volunteers (n = 10).

Repeatability data in healthy volunteers (n = 10)					
	Sequence	Meas.	Lipid	Creatine	Choline
Inter-subject coefficient of variation (σ_i^2)	STEAM-WET-150	150	37 %	24 %	86 %
	PRESS-WSC	60	52 %	10 %	53 %
Intra-subject coefficient of variation (σ_w^2)	STEAM-WET-150	150	26 %	21 %	23 %
	PRESS-WSC	60	19 %	5 %	6 %
Coefficient of repeatability	STEAM-WET-150	150	0.22 %	15.1 μmol / g	3.20 μmol / g
	PRESS-WSC	60	0.24 %	4.19 μmol / g	1.92 μmol / g

Table 3: Power calculations shows the number of subjects (N) *needed to determine statistical significance (power = 95%, α = 0.05) for a 20% change in concentration for each metabolite using STEAM-WET-150 (150 measurements) and PRESS-WSC (60 measurements). The calculations assume that only 60% of the subjects have quantifiable spectra.*

	STEAM-WET-150	PRESS-WSC
No. measurements	150	60
Scan duration	~ 30 minutes	~ 10 minutes
Numbers needed for paired studies assuming 60% 'success' rate in acquisition power = 95%, α = 0.05		
Lipid	42	49
Creatine	24	7
Choline	17	9